



CHORUS

This is the accepted manuscript made available via CHORUS. The article has been published as:

Thermoelectric properties of AgGaTe_2 and related chalcopyrite structure materials

David Parker and David J. Singh

Phys. Rev. B **85**, 125209 — Published 30 March 2012

DOI: [10.1103/PhysRevB.85.125209](https://doi.org/10.1103/PhysRevB.85.125209)

Thermoelectric properties of AgGaTe₂ and related chalcopyrite structure materials

David Parker and David J. Singh

Oak Ridge National Laboratory, 1 Bethel Valley Rd., Oak Ridge, TN 37831

(Dated: March 15, 2012)

We present an analysis of the potential thermoelectric performance of p-type AgGaTe₂, which has already shown a ZT of 0.8 with partial optimization, and observe that the same band structure features, such as a mixture of light and heavy bands and isotropic transport, that lead to this good performance are present in certain other ternary chalcopyrite structure semiconductors. We find that optimal performance of AgGaTe₂ will be found for hole concentrations between 4×10^{19} and $2 \times 10^{20} \text{cm}^{-3}$ at 900 K, and 2×10^{19} and 10^{20}cm^{-3} at 700 K, and that certain other chalcopyrite semiconductors might show good thermoelectric performance at similar doping ranges and temperatures if not for higher lattice thermal conductivity.

I. INTRODUCTION

Thermoelectric performance, as characterized by the so-called figure of merit, ZT , is a property of matter that has attracted much recent interest. The expression for ZT is $ZT = \sigma S^2 T / \kappa$, where S is the thermopower, T is temperature, σ is electrical conductivity and κ is the thermal conductivity, typically written as the sum of lattice and electronic contributions, $\kappa = \kappa_l + \kappa_e$. Obtaining high ZT is a fundamental scientific challenge, since high ZT is a strongly counter-indicated transport property. Specifically, one requires (1) high mobility at the same time as low thermal conductivity, suggesting weak scattering of charge carriers, but strong scattering of phonons, (2) high conductivity and high thermopower, (3) low thermal conductivity (i.e. soft lattice) and high melting point, and finally (4) the combination of heavy band behavior (for high S) at the same time as effective controlled doping. Although there is no known fundamental limit on ZT , for many decades the maximum known ZT in any material was near 1.0, while in recent years new concepts such as the use of nanostructuring^{1,2} or ‘rattling’³⁻⁵ to reduce thermal conductivity, and complex or modified electronic structure (e.g. by nanoscale effects⁶, or selection of materials with unusual band structures^{4,7,8}) have raised the best ZT values to near 2. Reviews of the field may be found in Refs. 9 and 10.

Here we discuss AgGaTe₂ and related chalcopyrite compounds, which we find to have unusual band structures combining heavy and light features that represent one route for resolving the above conundrums, particularly those relating to electrical conductivity and thermopower. An early study of chalcopyrite band structures is found in Ref. 11.

While heavy mass bands are generally favorable towards producing high thermopower, an essential ingredient for thermoelectric performance, such bands also generally reduce the carrier mobility and conductivity, so that very heavy mass bands on their own are not universally beneficial for good thermoelectric performance (i.e. ZT). Light mass bands, by contrast, are favorable for electrical conductivity but not so for thermopower. However, a *mixture* of light and heavy bands has previously been shown to be beneficial for thermoelectric performance¹², with the light band providing good conduction and the heavy band a small energy scale helpful for the thermopower. The telluride La₃Te₄ is a good example¹³ of a high performance material in which this behavior is realized. An

explanation of the role of a heavy band - light band mixture in transport is contained in the Appendix.

Combining heavy and light bands near the band edge is one example of a complex band structure affecting transport. As stated above, in general thermoelectric performance is a counter-indicated property, requiring high thermopower (connected with heavy bands) and high mobility (normally associated with light bands). Other examples of complex band structures affecting thermoelectric performance include the complex band structure of Na_xCoO₂¹⁴⁻¹⁶ and the associated ‘pudding mold’ band shape^{17,18}, and the modification of band structure by resonant levels¹⁹.

AgGaTe₂ has already shown a ZT of 0.8 at 850 K²⁰ at a low hole doping of approximately 10^{16}cm^{-3} , far outside the heavy doping ranges of 10^{19} - 10^{21}cm^{-3} where optimal performance is typically found in thermoelectrics. Structurally, it is very different from the chemically related compounds, PbTe and AgSbTe₂, as it is tetrahedrally bonded, rather than octahedral. We show that the valence band electronic structure of this *p*-type material is very similar to that of certain other ternary chalcopyrite semiconductors, which also show two factors favorable for thermoelectric performance - nearly isotropic transport and a mixture of heavy and light bands. The nearly isotropic transport arises from the (well known) similarity of the chalcopyrite physical structure of these materials and the cubic zincblende structure, as described above. We depict the chalcopyrite structure of AgGaTe₂ in Figure 1.

II. MODEL, CALCULATED BANDSTRUCTURES AND DENSITY-OF-STATES

In order to study the transport in AgGaTe₂ and related materials quantitatively, we employ first principles density-functional theory as implemented in the linearized augmented plane-wave (LAPW) WIEN2K code²¹. Since first principles methods often significantly understate the band gap, we here employ a modification of the generalized gradient approximation (GGA) due to Tran and Blaha²² known as a modified Becke Johnson potential²³, which has been shown to give much more accurate band gaps than the standard GGA. All calculations were performed to self-consistency to an accuracy of better than one meV per unit cell, using between 1000 and 2000 *k*-points in the full Brillouin zone, with spin-orbit coupling included for all materials except for

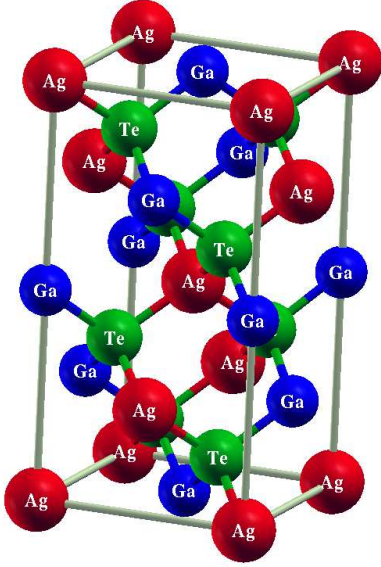


FIG. 1. (Color online). The physical structure of AgGaTe_2 . The planar lattice constant is 6.23 \AA and the c -axis value 11.96 \AA for a c/a ratio of 1.92.

ZnSiAs_2 . For AgGaTe_2 , internal coordinates were optimized, using the Perdew-Burke-Ernzerhof²⁴ GGA. To calculate the thermopower, as well as the conductivity anisotropy, we used the Boltzmann transport code BOLTZTRAP²⁵ within the constant scattering time approximation (CSTA). In this approximation, the scattering time of an electron is assumed to depend only on doping and temperature, but not the *energy* of the electron. When employed within the canonical expressions for the thermopower and conductivity, as given in Ref. 26, this results in expressions - the thermopower S and the conductivity anisotropy $\sigma_{\text{planar}}/\sigma_{c\text{-axis}}$ - with *no* dependence on any assumed absolute value of the scattering time. The CSTA has been used with quantitative success to describe the thermopower of a large number of thermoelectric materials²⁷⁻³⁶. Its quantitative success is the principal reason for its continued usage, although introducing an energy dependence to the scattering time (as for example, is theorized to occur with acoustic phonon - electron scattering) would typically have only a minimal decrease on the calculated thermopower. Perhaps the situation wherein the CSTA might be likelier to experience difficulties is in bipolar (double sign) conduction, where the assumption that the valence and conduction bands have equal scattering times can be debated. In such situations, however, thermoelectric performance is typically greatly reduced and so these situations are of little practical interest.

With regards to bipolar conduction, this typically can become an issue when the temperature (literally $k_B T$, where k_B is Boltzmann's constant) is greater than approximately a sixth of the band gap value, as noted by Mahan³⁷, although this is only a rough qualitative guide; recent work of ours on CrSi_2 ³⁸ suggests that this material may experience good thermoelec-

tric performance, free from bipolar effects, at temperatures of 1250 K, or roughly a third of the band gap. Clear signatures of bipolar conduction are, for given carrier concentration (as in an experiment), thermopower *decreasing* with increasing temperature. Such a decrease is often accompanied by an *increase* in the electronic component of thermal conductivity which is detrimental to thermoelectric performance. At fixed temperature (as in several of the subsequent plots) a signature of bipolar conduction is a *reduction* in the absolute value of the thermopower with *decreasing* concentration. This is the reverse of the usual situation in which thermopower *increases* with decreasing carrier concentration.

As is well-known, in the low temperature limit the thermopower is proportional to the temperature, which can be seen from the expression for the thermopower (here $\sigma(E)$ is the transport function, $N(E)$ $v(E)$ and $\tau(E)$ are the density of states, Fermi velocity and scattering time, respectively; f the Fermi function)

$$S(T) = \frac{\int_{-\infty}^{\infty} dE \sigma(E) (E - \mu) \partial f / \partial E}{\int_{-\infty}^{\infty} dE \sigma(E) \partial f / \partial E} \quad (1)$$

$$\sigma(E) = N(E) v^2(E) \tau(E) \quad (2)$$

It is clear from Eq. 1 that the thermopower must vanish at $T=0$, and expansion of the derivative of the Fermi function using the Sommerfeld expansion and an integration by parts yields the T-linear behavior. For higher temperatures the derivative of the Fermi function broadens in energy and the thermopower becomes a complex function of the band structure.

We begin with the band structure, previously considered in Ref. 39. Depicted in Figure 2 is the calculated bandstructure of AgGaTe_2 within the tetragonal Brillouin zone⁴⁰. The calculated band gap, at 1.15 eV, falls in the center of the 0.9 - 1.3 eV range of band gap values found in the literature⁴¹⁻⁴⁸, and is sufficient to prevent bipolar conduction at temperatures of 900 K and below.

Both the valence band maximum (VBM) and conduction band minimum (CBM) are located at the Γ point. These pockets generally show a fair degree of isotropy, with the dispersion somewhat greater along the Γ -Z line than the planar Γ -N direction. Of interest for the thermoelectric performance, the plot depicts a mixture of heavy and light bands near the VBM. The heavy band shows a Γ -N dispersion of 0.7 eV, leading to an approximate band mass of $1 m_0$, with the light band at roughly half this mass. As stated previously, this light-band/heavy band combination has previously been shown to be good for thermoelectric performance¹².

In Figure 3 we present the calculated density-of-states. The heavy valence band's impact is immediately apparent, with the DOS rising rapidly just below the VBM. A similarly heavy band appears somewhat above the CBM, with a highly dispersive band (inset) in the first 0.25 eV above the CBM. Also presented in Figure 3 is the atom-projected DOS. It is worth noting that for all atoms and both the VBM and CBM, the relevant atomic character is of virtually the same shape as the overall DOS, suggesting a coherence to the electronic scattering which tends to affirm the accuracy of the CSTA.

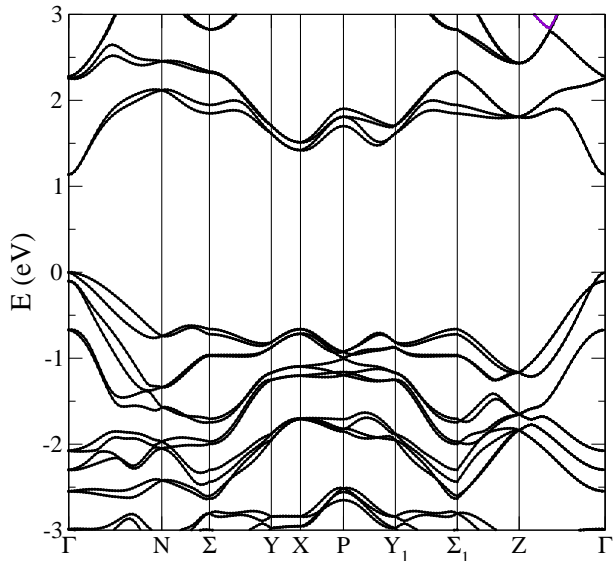


FIG. 2. The calculated bandstructure of AgGaTe_2 . The zero of energy is set to the valence band maximum.

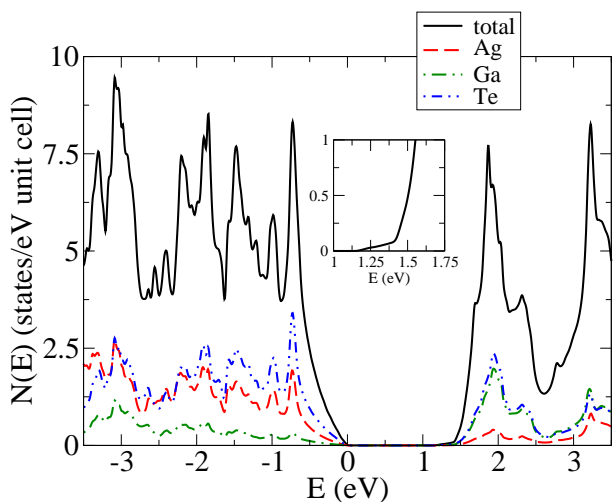


FIG. 3. (Color online). The density of states of AgGaTe_2 . The zero of energy is set to the valence band maximum. Inset: the density of states near the conduction band minimum.

III. CALCULATED THERMOPOWER AND CONDUCTIVITY RESULTS

In Figure 4 we depict the calculated hole-doped thermopower results for AgGaTe_2 . The plot depicts (at 700 and 900 K, the maximum operation temperature for AgGaTe_2) an essentially logarithmic dependence of thermopower on carrier concentration, in line with Pisarenko behavior. No effects of bipolar conduction are visible, and the plot shows 900 K thermopowers (virtually isotropic as described in Section 1) approaching $400 \mu\text{V/K}$ at hole concentrations p of $2 \times 10^{19} \text{cm}^{-3}$. Given the lack of information regarding the hole mobility at these concentrations and temperatures, estimating the figure-

of-merit ZT at these temperatures is impractical. We can say, however, that in previously studied materials thermoelectric performance is typically optimum for thermopowers between $200\text{-}300 \mu\text{V/K}$. Note that the Wiedemann-Franz relationship implies that, even if the lattice thermal conductivity were nil, a thermopower of $156 \mu\text{V/K}$ would be required to attain a ZT of unity (the typical minimum value for a material to be considered a “high performance thermoelectric”), so that in practice thermopowers substantially above this value are necessary to achieve high performance.

At 900 K for AgGaTe_2 these $200\text{-}300 \mu\text{V/K}$ thermopowers are found for hole concentrations between 4×10^{19} and $2 \times 10^{20} \text{cm}^{-3}$; at 700 K these thermopowers are found for concentrations between 2×10^{19} and 10^{20}cm^{-3} . While we cannot make a definite estimate of ZT , we can say with high confidence that performance substantially above the $0.8 ZT$ value achieved in Ref. 20 will be found. We assert this because the sample in this reference was sufficiently underdoped as to yield a thermopower which *decreased* with increasing temperature from 300 K all the way to the highest temperature measured, strongly indicative of bipolar conduction (always unfavorable for thermoelectric performance). Our results here show bipolar conduction can be avoided by heavy doping while maintaining high thermopower.

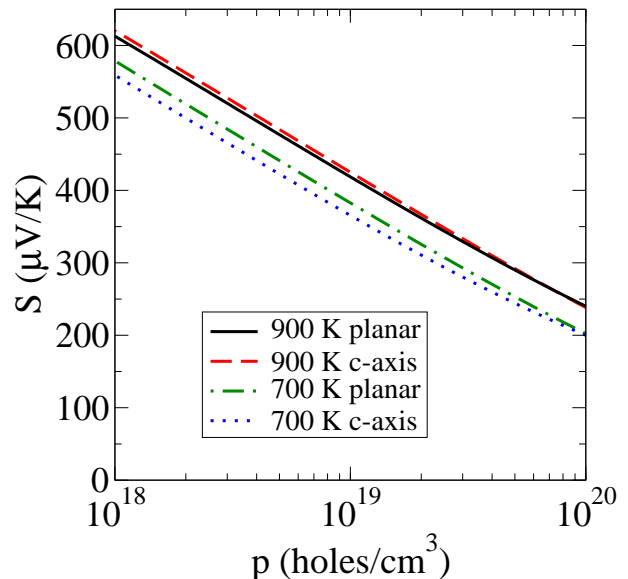


FIG. 4. (Color online). The calculated hole-doped thermopowers of AgGaTe_2 at 700 and 900 K.

Although experimental work to date has found that AgGaTe_2 tends to form p -type, in Figure 5 we present the calculated electron doped thermopower. Somewhat lower values than in the hole-doped case are apparent due to the increased dispersion on the electron-doped side, but the values depicted are still substantial. In addition, as with the valence bands the conduction bands contain a mixture of heavy and light bands, beneficial for thermoelectric performance. Finally, although the thermopower is lower than for hole doping, this can be partly compensated for by the likely increased mobility for

electron doping. We therefore expect that good performance may obtain for electron doping, in the range of $1.5 \times 10^{19} - 10^{20} \text{ cm}^{-3}$ at 900 K and $3 \times 10^{18} - 2 \times 10^{19} \text{ cm}^{-3}$ at 700 K (using the same criteria as for hole doping).

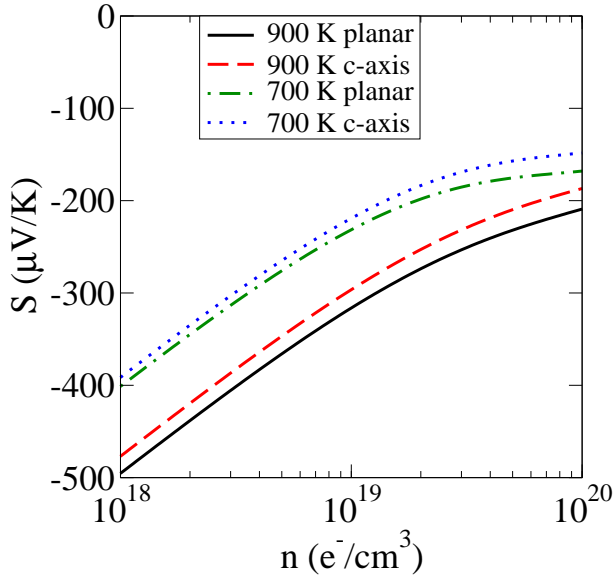


FIG. 5. (Color online). The calculated electron-doped thermopowers of AgGaTe₂ at 700 and 900 K.

In Figure 6 we depict the hole-doped thermopower at 300 K. This shows similarly favorable behavior to the high-temperature results, albeit with lower values. Somewhat greater anisotropy than in the high temperature case is apparent, due mainly to the narrower energy range of the valence band that is relevant for transport at these lower temperatures. This can be seen more directly from looking at the band structure plot (Fig. 2) - the band mass of the light band in the Γ -Z direction is roughly one half the mass of the heavy band in the Γ -N direction. At low dopings and temperatures (such as 300 K), for c-axis transport it is only this light band that is operative in transport and there is therefore substantial anisotropy in the calculated thermopower. As one moves to heavier dopings the heavier band (whose maximum is roughly 100 meV below the VBM) becomes operative and yields substantially more isotropic behavior. We note also that both planar and c-axis thermopower obey a Pisarenko type relationship (i.e. logarithmic in carrier concentration) at the low dopings, indicative of non-degenerate single band transport, and deviate from this at higher dopings, due both to the two band behavior and the approaching of the degenerate limit. In Figure 7 we present the 900 K conductivity anisotropy, which is essentially nil, a significant advantage for applications, as discussed previously.

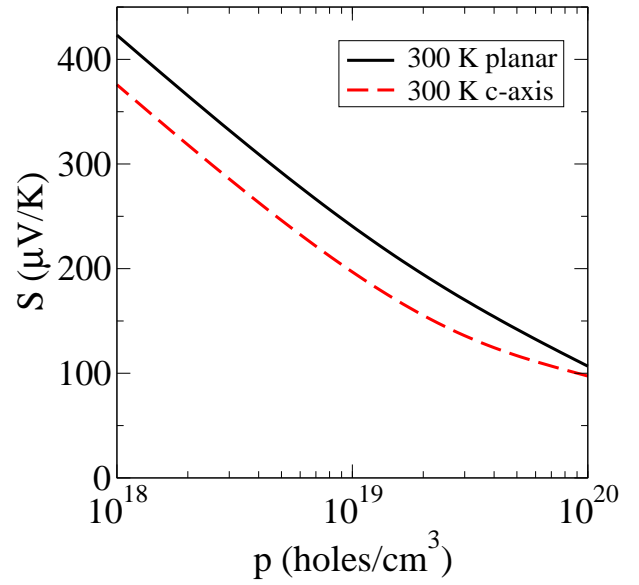


FIG. 6. (Color online). The calculated hole-doped thermopowers of AgGaTe₂ at 300 K.

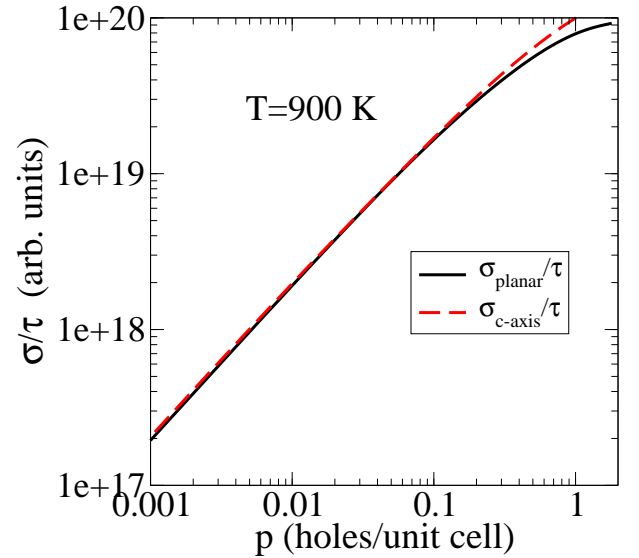


FIG. 7. (Color online). The calculated electrical conductivity (divided by scattering time) of AgGaTe₂ at 900 K. Note that one hole per unit cell is equivalent to $4.31 \times 10^{21} \text{ cm}^{-3}$.

IV. OBSERVATION ON VALENCE BAND STRUCTURE IN TERNARY CHALCOPYRITE SEMICONDUCTORS AND THERMOPOWER OF CDGEAS₂

In this section we point out that there are a number of ternary chalcopyrite semiconductors with nearly the same physical and electronic structure as AgGaTe₂ that can be expected to give similarly beneficial Seebeck coefficients and isotropic electronic conductivity. To illustrate the point in Figure 8 we present the calculated band structure of *six* different chalcopyrite structure semiconductors, including AgGaTe₂.

For simplicity we limit ourselves to the valence band structure as most, if not all these compounds generally behave as p-type semiconductors. We note firstly that in all these compounds the valence band maximum is centered at Γ (note that the plots are scaled so that within a given plot, momentum space distances between labeled points are proportional to the distance along the x-axis). The plots also indicate a general consistency of dispersive energy scales - for all of the plots the Γ -N dispersion is between 0.4 and 0.8 eV and that in the Γ -Z direction between 0.75 eV and 1.2 eV. While the plot-to-plot differences increase at greater distances (> 1 eV) from the VBM, for the purposes of transport consideration these are of little importance.

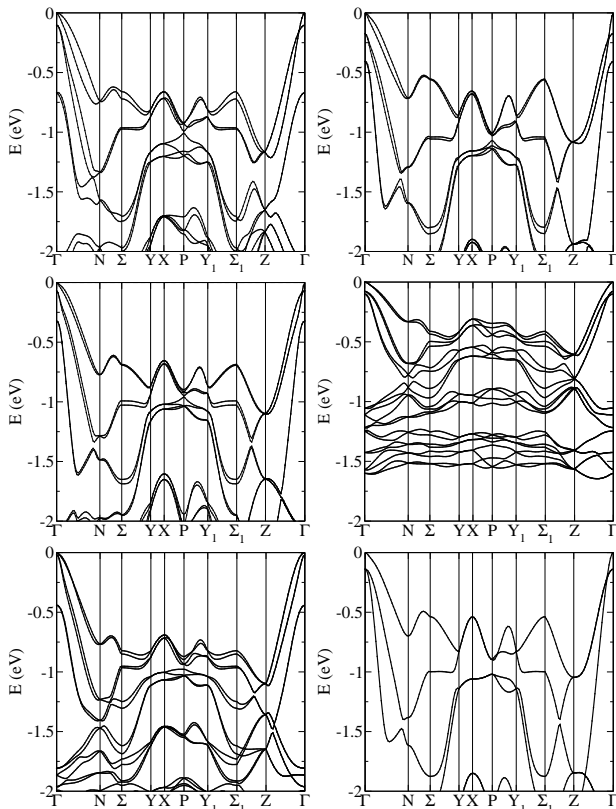


FIG. 8. The calculated valence band structures of (top left) AgGaTe₂; top right CdGeAs₂; middle left CdSnAs₂; middle right CuInS₂; bottom left CuInTe₂; bottom right ZnSiAs₂.

As with AgGaTe₂, these valence band plots generally contain a mixture of heavy and light bands. This has previously been shown^{12,13} to be good for thermoelectric performance. However, the lattice thermal conductivity (presented in Table 1) of most of these materials is much higher than that of AgGaTe₂, making them generally less favorable for thermoelectric performance. To the degree that this lattice term can be reduced by alloying and nanostructuring, these materials may show good performance as well. Given the large number of materials with very similar electronic structure, we would expect that alloying these materials with each other should be possible and effective at reducing $\kappa_{lattice}$. We note (Table 1) that for these materials, with the exception of CdSnAs₂, the

TABLE I. Lattice thermal conductivity $\kappa_{lattice}$ at 300 K and experimental band gaps of chalcopyrite compounds. Thermal conductivity (taken for polycrystalline samples) from Ref. 49, and band gaps from Ref. 52, except where noted.

Compound	$\kappa_{lattice}$ (W/m K)	Band gap (eV)
AgGaTe ₂	1.7 ²⁰	1.15
CdGeAs ₂	4.0	0.57
CdSnAs ₂	7.5	0.26 ⁵⁰
CuInS ₂	12.5 ⁵¹	1.53
CuInTe ₂	5.5	0.98
ZnSiAs ₂	14.0	1.92

experimental band gap is sufficiently large to prevent bipolar conduction at temperatures below 900 K, so that the assessment of favorable valence band structure implies good thermopower behavior as well.

Perhaps the likely best performer of the remaining five materials would be CdGeAs₂ with its 300 K lattice thermal conductivity listed in Ref. 49 as 4 W/m-K. In Figure 9 we present the calculated 900 K hole-doped thermopower (the melting point is 943 K) of this material, noting that even at the relatively high hole doping of 10^{20}cm^{-3} the thermopower is still over $250 \mu\text{V/K}$, an excellent value for thermoelectric performance, particularly since the lattice term at this temperature (assuming a canonical $1/T$ behavior) would be just 1.3 W/m-K.

Included in the plot are two calculated curves - one assuming the first principles calculated band gap of 0.65 eV, and a results assuming a somewhat smaller gap of 0.5 eV. We have included the additional curve because there is evidence⁵² that the band gap of CdGeAs₂ decreases significantly with temperature. For both curves, as with the AgGaTe₂ the concentration dependence is essentially logarithmic at high dopings, until one approaches the bipolar regime where the thermopower decreases with decreasing concentration. For the as-calculated gap of 0.65 eV this happens for $p = 3 \times 10^{18}\text{cm}^{-3}$; for the smaller gap this happens at 10^{19}cm^{-3} . Using the same criteria as for AgGaTe₂ we find that optimal doping will most likely be found for hole concentrations between 5×10^{19} and $2 \times 10^{20}\text{cm}^{-3}$, and this statement is independent of the value taken for the band gap. We note also that in the non-bipolar regime (i.e. to the right of the thermopower maximum in Figure 9) the thermopower is very similar to that of AgGaTe₂, as would be expected given the similar electronic structure.

Although we have not calculated the thermopower of the remaining materials, to the extent that the dispersive energy scales are similar to those of AgGaTe₂ and CdGeAs₂ the thermopower will be similar as well. CuInS₂, in particular, may well have even larger thermopower than these materials given the smaller Γ -N and Γ -Z dispersions; actual performance of this material, however, is expected to be low due to the high lattice thermal conductivity and likely low mobility of this sulfide; the same considerations apply to ZnSiAs₂.

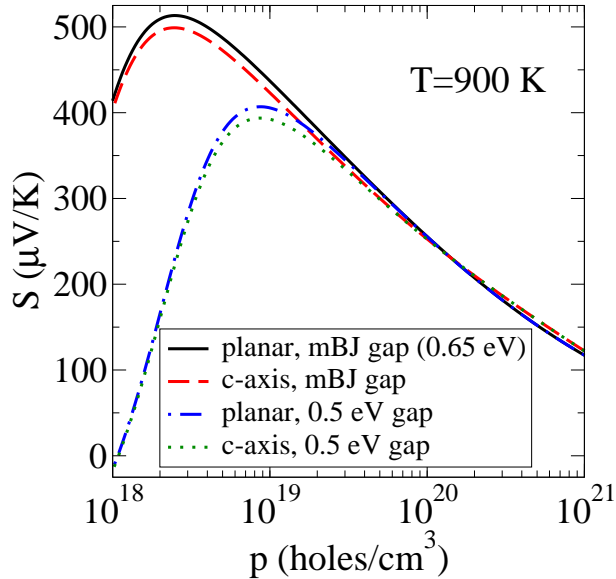


FIG. 9. (Color online). The calculated hole-doped thermopower of CdGeAs₂ at 900 K.

V. CONCLUSION

To conclude, in this work we have shown that the ternary chalcopyrite semiconductor AgGaTe₂ may show excellent thermoelectric performance at hole dopings ranging from 4×10^{19} and $2 \times 10^{20} \text{cm}^{-3}$ at 900 K and between 2×10^{19} and 10^{20}cm^{-3} at 700 K. This performance may well be due to a heavy-band light-band structure near the valence band maximum and will be aided by nearly isotropic transport. In addition, we have shown that the valence band structure of this material is very similar to that of a number of ternary chalcopyrite semiconductors, which might therefore show good thermoelectric performance if not for a relatively high lattice thermal conductivity. Given the general alloying capability of chalcopyrite semiconductors, it may be of interest to pursue heavy doping of these materials in concert with alloying with other chalcopyrite materials.

Acknowledgments

DJS is grateful for helpful discussions on tetrahedrally bonded thermoelectric materials with X. Shi, Lili Xi, Jiong Yang and Wenqing Zhang. This research was supported by the U.S. Department of Energy, EERE, Vehicle Technologies, Propulsion Materials Program (DP) and the Solid State Solar-Thermal Energy Conversion Center (S3 TEC), an Energy Frontier Research Center funded by the US Department of Energy, Office of Science, Office of Basic Energy Sciences under Award Number: DE-SC0001299/DE-FG02-09ER46577 (DJS).

VI. APPENDIX: EXPLANATION OF FAVORABILITY OF HEAVY BAND - LIGHT BAND MIXTURE

In this section we give an explanation for the favorable thermoelectric properties of a heavy band light band mixture. Consider a system with two parabolic bands of effective masses m_1 and m_2 . For simplicity we will assume that they are degenerate in energy at the valence band maximum, work at low temperature in which the Mott formula is valid, and consider the behavior of the power factor $S^2\sigma(T)$ in two relevant situations, relative to the case in which there is only a single band. To ensure a fair comparison these situations will be the following: the Fermi energy in the two band case is the same as in the one band case; and the carrier concentration in these two situations is the same. To begin, we recall the Mott formula, given as (neglecting factors of k_B , \hbar and e , the electron charge)

$$S(T) = \frac{\pi^2}{3} T \left(\frac{d\sigma(E)/dE}{\sigma(E)} \right)_{|E=E_F} \quad (3)$$

We shall assume that the scattering time τ is constant throughout the following analysis. For a single parabolic band the logarithmic derivative in the previous expression reduces to $3/2E_F$, and a quick check reveals that this relationship holds in the case of *two* (or more) degenerate parabolic bands. This implies that in the situation wherein the two band E_F is the same as the one band, the thermopower is unchanged, and since the electrical conductivities of the two bands add linearly the power factor is clearly enhanced by the addition of the extra band.

The second situation, in which carrier concentration is assumed to be the same in the single and two band cases, requires somewhat more work to analyze due to the change of the Fermi energy from the single band case to the two band case. Consideration of the $T=0$ limit of the carrier concentration by integrating the density of states yields the following result, valid for two parabolic bands:

$$E_F = A \left(\frac{3n}{2} \right)^{2/3} \left[m_1^{3/2} + m_2^{3/2} \right]^{-2/3} \quad (4)$$

where A is a constant independent of carrier concentration, energy or the masses. Similarly, for two parabolic bands the transport function can be written as

$$\sigma(E) = BE^{3/2} (m_1^{1/2} + m_2^{1/2}) \quad (5)$$

with B a constant. Combining the previous two expressions in the low-temperature limit in which $E \rightarrow E_F$, we find that

$$\sigma(E_F) = C \frac{3n m_1^{1/2} + m_2^{1/2}}{2 m_1^{3/2} + m_2^{3/2}} \quad (6)$$

Here C is a constant independent of the band masses, temperature and concentration. One may readily see, by imagining m_1 to be the mass in the single band case, that if $m_2 < m_1$ the transport function, and hence electrical conductivity, *increase* via the addition of the second band, while the reverse is true

if $m_2 > m_1$. This second result is made reasonable by considering that at fixed carrier concentration one is essentially asking about the effect of the second band on electrical *mobility*, and it is clear that if the second (degenerate in energy) band is heavier than the first the mobility will decrease.

It is possible to show, however, that even in this last case, and in fact regardless of the mass of the second band, the *power factor* $S^2\sigma(T)$ will increase as a result of the addition of the second band. To see this we write S , using the Mott relation for parabolic bands presented earlier, as

$$S(T) = \frac{\pi^2}{2} T/E_F \quad (7)$$

and substitute previous expressions for E_F to find finally

$$S^2(T)\sigma(E_F) = DT^2 \left(\frac{2}{3n}\right)^{1/3} (m_1^{3/2} + m_2^{3/2})^{1/3} (m_1^{1/2} + m_2^{1/2}) \quad (8)$$

where D is a constant independent of the band masses, temperature and concentration. In this expression the effect of m_2 is found to be an increase regardless of its value; the increase of $S^2(T)$ as a result of adding the second band, whether heavy or light, outstrips the decrease in mobility if $m_2 > m_1$, and is supported by an increase in mobility if $m_1 > m_2$. For

simplicity we have here taken the electrical conductivity $\sigma(T)$ at low temperature to be $\sigma(E_F)$, the transport function evaluated at the zero temperature Fermi energy, which holds in the same regime in which the Mott relation is valid. We note also that the above expression implies that for a given m_1 , a larger m_2 , signifying a heavier band, increases thermoelectric performance more than a band of the same mass would, suggesting the beneficial effect of heavier band mass. Finally, for sufficiently small doping the range of temperature in which the expressions for S and $\sigma(T)$ are valid shrinks rapidly. In particular, the power factor $S^2\sigma$ does *not* diverge as $n \rightarrow 0$, as implied by Eq. 6, since one then approaches the non-degenerate limit (in which Pisarenko behavior, $S \sim -\log(n)$, applies) at arbitrarily low temperature.

It should be stated that all of these calculations assume that the electron relaxation time does not vary when either the Fermi energy or carrier concentration is held constant (as the second band is “added”), and the accuracy of this assumption can reasonably be debated. Therefore the previous argument should be considered as a plausible explanation for the observed behavior - the beneficial nature of heavy-light band structures - rather than as a rigorous argument proving that these band structures are good for thermoelectric performance.

-
- ¹ B. Poudel, Q. Hao, Y. Ma, Y. Lan, A. Minnich, B. Yu, X. Yan, D. Wang, A. Muto, D. Vashaee, X. Chen, J. Liu, M. S. Dresselhaus, G. Chen, and Z. Ren, *Science* **320**, 634 (2008).
 - ² W. Xie, X. Tang, Y. Yan, Q. Zhang and T.M. Tritt, *Appl. Phys. Lett.* **94**, 102111 (2009).
 - ³ B.C. Sales, D. Mandrus and R.K. Williams, *Science* **272**, 1325 (1996).
 - ⁴ T. He, J. Chen, H.D. Rosenfeld and M.A. Subramanian, *Chem. of Mat.* **18**, 759 (2006).
 - ⁵ X. Shi, S. Bai, L. Xi, J. Yang, W. Zhang, L. Chen and J. Yang, *J. Mat. Res.* **26**, 1745 (2011).
 - ⁶ L.D. Hicks and M.S. Dresselhaus, *Phys. Rev. B* **47**, 12727 (1993).
 - ⁷ H. Wang, Y. Pei, A. D. LaLonde and G.J. Snyder, *Adv. Mat.* **23**, 1367 (2011).
 - ⁸ K. F. Hsu, S. Loo, F. Guo, W. Chen, J.S. Dyck, C. Uher, T. Hogan, E.K. Polychroniadis and M. G. Kanatzidis *Science* **303**, 818 (2004).
 - ⁹ G.J. Snyder and E.S. Toberer, *Nat. Mat.* **7**, 105 (2008).
 - ¹⁰ M.S. Dresselhaus, G. Chen, M.Y. Tang, R.G. Yang, H. Lee, D.Z. Wang, Z.F. Ren, J.-P. Fleurial and P. Gogna, *Adv. Mat.* **19**, 1043 (2007).
 - ¹¹ J.E. Jaffe and A. Zunger, *Phys. Rev. B* **30**, 741 (1984); **28**, 5822 (1983).
 - ¹² D. J. Singh and I. I. Mazin, *Phys. Rev. B* **56**, R1650 (1997).
 - ¹³ A.F. May, D.J. Singh and G.J. Snyder, *Phys. Rev. B* **79**, 153101 (2009).
 - ¹⁴ D.J. Singh, *Phys. Rev. B* **61**, 13397 (2000).
 - ¹⁵ D.J. Singh and D. Kasinathan, *J. Elec. Mat.* **36**, 736 (2007).
 - ¹⁶ H.J. Xiang and D.J. Singh, *Phys. Rev. B* **76**, 195111 (2007).
 - ¹⁷ K. Kuroki and R. Arita, *J. Phys. Soc. Jpn.* **76**, 083707 (2007).
 - ¹⁸ P. Wissgott, A. Toschi, G. Sangiovanni and K. Held, *Phys. Rev. B* **84**, 085129 (2011).
 - ¹⁹ J.P. Heremans, V. Jovic, E.S. Toberer, A. Saramat, K. Kurosaki, A. Charoenphakdee, S. Yamanaka and G.J. Snyder, *Science* **321**, 554 (2008).
 - ²⁰ A. Yusufu, K. Kurosaki, A. Kosuga, T. Sugahara, Y. Ohishi, H. Muta and S. Yamanaka, *Appl. Phys. Lett.* **99**, 061902 (2011).
 - ²¹ P. Blaha, K. Schwarz, G. K. H. Madsen, D. Kvasnicka and J. Luitz, WIEN2k, An Augmented Plane Wave + Local Orbitals Program for Calculating Crystal Properties (Karlheinz Schwarz, Techn. Universität Wien, Austria), 2001. ISBN 3-9501031-1-2.
 - ²² F. Tran and P. Blaha, *Phys. Rev. Lett.* **102**, 226401 (2008).
 - ²³ A. D. Becke and E. R. Johnson, *J. Chem. Phys.* **124**, 221101 (2006).
 - ²⁴ J. P. Perdew, K. Burke, and M. Ernzerhof, *Phys. Rev. Lett.* **77**, 3865 (1996); **78**, 1396 (1997).
 - ²⁵ G.K.H. Madsen, K. Schwarz, P. Blaha and D.J. Singh, *Phys. Rev. B* **68**, 125212 (2003).
 - ²⁶ J. M. Ziman, *Principles of the Theory of Solids*, (Cambridge: 1999).
 - ²⁷ D.J. Singh, *Phys. Rev. B* **81**, 195217 (2010).
 - ²⁸ D. Parker and D.J. Singh, *Phys. Rev. B* **82**, 035204 (2010).
 - ²⁹ L. Zhang, M.-H. Du and D.J. Singh, *Phys. Rev. B* **81**, 075117 (2010).
 - ³⁰ K.P. Ong, D.J. Singh and P. Wu, *Phys. Rev. B* **83**, 115110 (2011).
 - ³¹ G. K. H. Madsen, K. Schwarz, P. Blaha, and D. J. Singh, *Phys. Rev. B* **68**, 125212 (2003).
 - ³² D. J. Singh and I. I. Mazin, *Phys. Rev. B* **56**, R1650, (1997).
 - ³³ T. J. Scheidemantel, C. Ambrosch-Draxl, T. Thonhauser, J. V. Badding, and J. O. Sofo, *Phys. Rev. B* **68**, 125210, (2003).
 - ³⁴ L. Bertini and C. Gatti, *J. Chem. Phys.* **121**, 8983, (2004).
 - ³⁵ L. Lykke, B. B. Iversen, and G. K. H. Madsen, *Phys. Rev. B* **73**, 195121, (2006).
 - ³⁶ Y. Wang, X. Chen, T. Cui, Y. Niu, Y. Wang, M. Wang, Y. Ma, and G. Zou, *Phys. Rev. B* **76**, 155127, (2007).
 - ³⁷ J.O. Sofo and G.D. Mahan, *Phys. Rev. B* **49**, 4565 (1994).

- ³⁸ D. Parker and D.J. Singh, under editorial review.
- ³⁹ A. H. Reshak, *Physica B* **369**, 245 (2005).
- ⁴⁰ M. Lax, *Symmetry Principles in Solid State and Molecular Physics*, (John Wiley: 1974), p. 449.
- ⁴¹ B. Tell, J.L. Shay and H.M. Kasper, *Phys. Rev. B* **9**, 5203 (1974).
- ⁴² R. Kumar and R.K. Bedi, *J. Mat. Sci.* **40**, 455 (2005).
- ⁴³ U.N. Roy, B. Mekonen, O.O. Adetunki, K. Chattopahhyay, F. Kochari, Y. Cui, A. Burger and J.T. Goldstein, *J. Cryst. Growth* **241**, 135 (2002).
- ⁴⁴ P.G. Schunemann, S.D. Setzler, T.M. Pollak, M.C. Ohmer, J.T. Goldstein and D.E. Zelmon, *J. Cryst. Growth* **211**, 242 (2000).
- ⁴⁵ S. Chatraphorn, T. Panmatarite, S. Pramatus, A. Prichavudhi, R. Kritayakirana, J. O. Berananda, V. Sayakanit and J.C. Woolley, *J. Appl. Phys.* **57**, 1791 (1985).
- ⁴⁶ S. Arai, S. Ozaki and S. Adachi, *Appl. Optics* **49**, 829 (2010).
- ⁴⁷ B.R. Pamplin, T. Kiyowasa and K. Masumoto, *Prog. Cryst. Growth Char.* **1**, 331 (1979).
- ⁴⁸ J. Shewchun, J.J. Loferski, R. Beaulieu, G.H. Chapman and B.K. Garside, *J. Appl. Phys.* **50**, 6978 (1979).
- ⁴⁹ D.P. Spitzer, *J. Phys. Chem. Sol.* **31**, 19 (1970).
- ⁵⁰ Our theoretical calculations find the band gap of this compound to be 0.44 eV, substantially larger than the experimental value.
- ⁵¹ L.A. Makovetskaya, I.V. Bodnar, B.V. Korzun, G.P. Yaroshevich, *Phys. Stat. Sol. A* **74**, K59 (1982).
- ⁵² Landolt Börnstein Database, Springer Materials, available online at www.springermaterials.com.